J Mater Sci: Mater Med (2006) 17: 517–521
DOI 10.1007/s10856-006-8934-2

Hydroxyapatite (HA) bone scaffolds with controlled macrochannel pores

Chang-Jun Bae · Hae-Won Kim · Young-Hag Koh · Hyoun-Ee Kim

Received: 6 May 2005 / Accepted: 9 August 2005

Abstract Hydroxyapatite (HA) macrochanneled porous scaffolds, with a controlled pore structure, were fabricated via a combination of the extrusion and lamination processes. The scaffold was architectured by aligning and laminating the extruded HA and carbon filaments. The macrochannel pores were formed by removing the carbon filaments after thermal treatments (binder removal and sintering). The porosity of the scaffolds was varied between 48 and 73% with a controlled pore size of ∼450 μm, by adjusting the fractions of HA and carbon filaments. As the porosity was increased from 48 to 73%, the compressive strength decreased from 11.5 to 3.2 MPa. However, the osteoblast-like cell responses on the scaffold, such as the proliferation rate and alkaline phosphatase (ALP) activity, were significantly enhanced as the porosity was increased.

1. Introduction

Hydroxyapatite (HA: $Ca_{10}(PO_4)_6(OH)_2$) has attracted a great deal of attention for hard tissue applications due to its high osteoconductivity and bioactivity [1–6]. Most in vivo studies have proven that the HA bonds directly with the host tissues and leads to complete osseointegration. For use as tissue scaffolds, HA has been engineered to mimic the 3-dimensional inorganic component of natural bone, providing the space and area necessary for vascularization and tissue regeneration [7–10]. Conventional techniques, such as the hydrothermal exchange process [4], the pyrolysis of organic particles [11–14] and the polyurethane sponge technique [14, 15] have shown some limitations in the control of various aspects of the pore configuration, such as the pore size, porosity, pore geometry and interconnectivity. On the other hand, the solid freeform fabrication (SFF) method has emerged as a way of creating a precisely controlled pore structure by means of a layer-by-layer, sequential building process [16–18]. Another approach is the extrusion process, in which the thermoplastic ceramic and fugitive filaments are aligned alternatively, and then the fugitive material is removed with thermal treatment, to produce a 3-directional macrochanneled structure [19].

In this study, by combining the extrusion process with lamination, we fabricated HA porous scaffolds with a well-defined pore configuration. In particular, the porosity was precisely controlled, and its effect on the mechanical and biological properties of the scaffolds was investigated. The significance of this study lies in the investigation of these properties in HA porous scaffolds with a well defined pore configuration and porosity.

2. Materials and methods

2.1. Fabrication of HA porous scaffold

Commercially available HA [$Ca_{10}(PO_4)_6(OH)_2$, Alfa Aesar Co., USA] powder was used as the starting material. The HA powder was calcined at 900°C for 1 h in air to improve its powder characteristics [20]. The calcined HA powder with 1 wt% stearic acid (Sigma-Aldrich Co., USA) was ball-milled in ethanol for 24 h using alumina balls as the milling media and then dried. Carbon black powder (Cabot Black Pearls BP-120; Cabot Corp., Boston, USA) was used as the fugitive material, which was removed later by thermal treatment.

C.-J. Bae · Y.-H. Koh · H.-E. Kim (✉)
School of Materials Science and Engineering, Seoul National University, Seoul, 151-742, Korea
e-mail: kimhe@snu.ac.kr

H.-W. Kim
Department of Dental Biomaterials, School of Dentistry, Dankook University, Cheonan, 330-714, Korea

Table 1 Pore configuration of the macrochanneled HA scaffolds with different degrees of porosity

Green body	HA filament size (μm)	600	500	400	300	200
	Carbon filament size (μm)	600	600	600	600	600
	Designed porosity (%)	50	55	60	67	75
Sintered body	Scaffold Porosity (%)	48	53	59	65	73
	Framework thickness (μm)	503 ± 6	405 ± 6	324 ± 5	243 ± 7	158 ± 8
	Macrochannel size (μm)	454 ± 16	458 ± 7	465 ± 4	436 ± 14	448 ± 9

The ceramic and fugitive powders were blended separately with ethylene ethyl acrylate (EEA 6182; Union Carbide, Danbury, CT) and isobutyl methacrylate (Rohm and Haas, Philadelphia, PA) resins at 110°C in a heated shear mixer (Jeong-sung Inc, Seoul, Korea). Processing aids were also added to ensure that the mixtures had a consistent viscosity. Once compounded, each thermoplastic compound was warm-pressed using a 24 mm cylindrical mold and extruded using one of the five square type orifices (600 × 600, 500 × 500, 400 × 400, 300 × 300 and 200 × 200 μm) at 145°C with a crosshead speed of 3 mm/min using a piston extruder (Jung-min Ind. Co., Korea). Two types of filaments (HA and carbon black) were aligned alternately and warm-pressed at 140°C with an applied load of 10 MPa to produce a filament sheet. The sheet was cut and bi-axially stacked into a 24 × 24 mm square mold, followed by warm-pressing at 160°C with 20 MPa, to create a 3-directionally interconnected structure. The porosity of the scaffold was varied from 48 to 74% by adjusting the initial fraction of the carbon black filament (600 × 600 μm) relative to the HA filament (various dimensions, as described above). The stacked green body was heat-treated to 700°C in air to burn out the binder and then to remove the carbon black. To avoid the formation of defects in the green body, the samples were heated slowly. After removal of the binder and carbon, the samples were densified at 1300°C for 1 h in air. Data on the pore configuration of the initial green body and final scaffolds are summarized in Table 1.

2.2. Characterization and mechanical test

The morphology of the macrochanneled HA scaffold was observed by optical microscopy (PMG3, Olympus, Tokyo, Japan) and scanning electron microscopy (SEM; JSM-6330, JEOL Technics, Tokyo, Japan). The phase of the sample was analyzed by X-ray diffraction (XRD; MXP18A-HF, MAC Science, Tokyo, Japan) patterns. The compressive strengths of the scaffolds, with dimensions of 4 × 4 × 6 mm, were measured using an Instron 5565 (Instron Corp., Canton, MA) at a crosshead speed of 0.05 mm/min. Both edges were impregnated with paraffin to avoid the edge effect.

2.3. In vitro cellular assay

The human osteosarcoma (HOS) cell line was used to assess the cellular behaviors on the fabricated scaffolds [15, 21].

The cells were cultured on the macrochanneled HA scaffolds with various porosities at a seeding density of 1×10^4 cells/ml for periods of 4 and 14 days in an incubator humidified with 5% CO_2/95% air at 37°C. For the purpose of comparison, a dense HA ceramic was also tested. After culturing for 4 days, the cell morphology on the HA scaffolds was observed using SEM, after fixation with glutaraldehyde (2.5%), dehydration with graded ethanols (70, 90 and 100%) and critical point drying. The cell viability was assessed using the MTT method [21]. After culturing the cells for 4 days, MTT was added to the samples and left for 4 h. The absorbance of the blue formazan product was detected at 570 nm using a microplate reader. The functional activity of the cells was evaluated by measuring the alkaline phosphatase (ALP) activity after culturing for 14 days [15, 21]. After trypsinization and centrifugation, the cell pellets were resuspended in 0.1% Triton X-100 and disrupted via a freezing/thawing process. The cell lysates were assayed colorimetrically using *p*-nitrophenyl phosphate as the substrate. The color product, *p*-nitrophenol, was read at 410 nm using a spectrophotometer.

Each set of tests was performed in triplicate. Statistical comparison was carried out by means of analysis of variance (ANOVA), and significance was considered at $p < 0.05$, $p < 0.005$ and $p < 0.001$.

3. Results and discussion

Fig. 1 shows the three-dimensional morphology of the HA/carbon green body (A) and its heat-treated samples with different porosities (B,C). This architecture of the green body was achieved by aligning the HA (bright area) and carbon black (dark area) filaments alternately to form a sheet, and then stacking the sheet bi-axially (Fig. 1A). The orientations of the filaments are marked as "0°" and "90°". The two kinds of filaments were successfully welded together, without any of the cracks or delaminations which are often created due to the incoherence of the thermoplastic compounds. The green body was heat-treated at 700°C, in order to burn out the binder and to remove the carbon black, and was then further sintered at 1300°C to densify the HA framework.

Figs 1B and C show the micrographs of the sintered HA scaffolds with porosities of 48 and 65%, respectively.

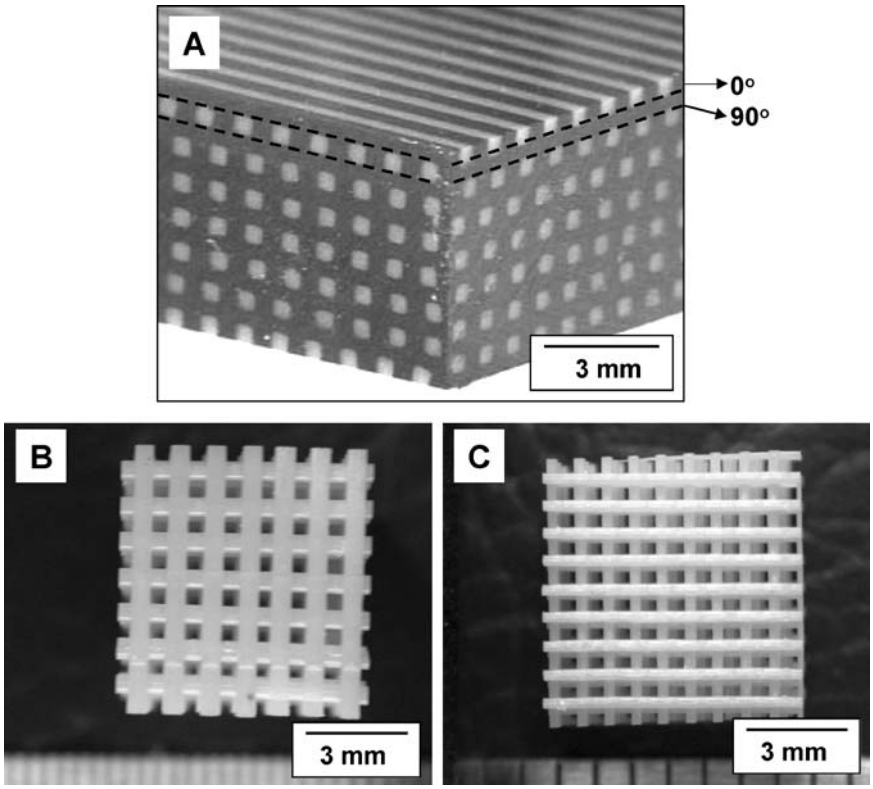

Fig. 1 Optical micrographs of the (A) HA/carbon black green body after being extruded and alternately laminated in the 0°/90° directions, and the macrochanneled HA scaffolds with porosities of (B) 48% and (C) 65% after sintering at 1300°C for 3 h in air. Bright and dark contrast in (A) represents thermoplastic HA and carbon black, respectively. Interconnected macrochannel pores in (B) were formed by removal of carbon black filament.

Macrochannels in a square shape, formed by the removal of the carbon black filaments, constituted a well-defined pore structure. The porosity increased from 48 to 73% as the thickness of the framework was decreased, while the macrochannel size remained almost constant (∼450 μm), as described in Table I. These results indicate that the hybrid extrusion and lamination process, using thermoplastic HA and carbon black filaments, provides an efficient method of controlling the porosity. Furthermore, the macrochannels were perfectly straight and interconnected. This large pore channel and high interconnectivity can provide an effective tunnel for blood circulation and cell anchorage and, ultimately, for bone growth into the scaffold [18–20].

On closer examination of the scaffold (Fig. 2(A)), the HA was found to be fully consolidated. The grain structure was typical of polycrystalline HA, as is usually observed in sintered bodies. This result indicates that the binders in the thermoplastic HA filament were completely removed, without generating any defects or preventing densification. The phase formed in the scaffold was confirmed to be pure HA by XRD pattern. Examination of the fracture surface of the scaffolds revealed the existence of good interfacial bonding between the filaments, with orientations of 0° and 90° (Fig. 2(B)).

The compressive strengths of the macrochanneled HA scaffolds with different degrees of porosity were measured, as shown in Fig. 3. As the porosity increased from 48 to 65%, the compressive strength gradually decreased from 11.5 to 3.2 MPa, and this was attributed to a reduction in the quantity of load-bearing HA framework. The scaffolds possessing higher porosities of over 70% were highly fragile and, thus, reliable data were difficult to obtain for these samples.

The biological properties of the macrochanneled HA scaffolds were assessed in terms of their osteoblast-like cell responses. The data were compared among the scaffolds with different degrees of porosity. All of the scaffolds showed similar cell growth morphology. A typical morphology of the cells, grown on the sample with culturing for 4 days, is shown in Fig. 4. The cell number and growth morphology on the framework of inside pore channels were similarly observed as those on the outermost surface region, suggesting the cells had migrated deep into the macrochannels during incubation. Moreover, the cell membranes were spread out in intimate contact with the HA surface.

The degree of cell viability on the scaffolds was estimated by means of the MTT assay, as shown in Fig. 5. The cell viability at day 4 increased gradually as the porosity increased, and those samples with porosities of 65 and 73% had significantly higher cell viability than that with the lowest porosity of 48%. This result was mainly attributed to the increased

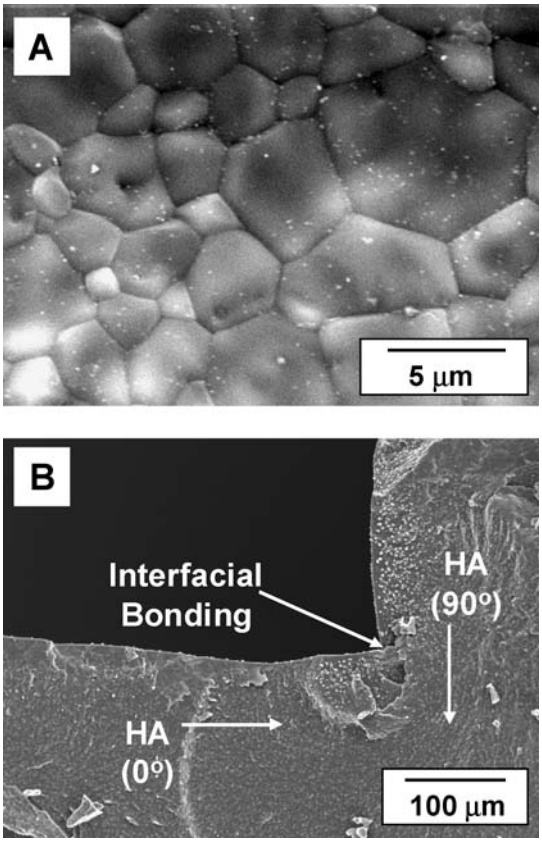

Fig. 2 SEM morphology of the HA framework; (A) as-sintered surface and (B) fractured surface. HA framework was fully densified without defects, and good interfacial bonding was obtained between the two HA frames with 0° and 90° alignments.

surface area associated with the increase in porosity and the consequent larger number of cells initially attached on the scaffold with higher porosity.

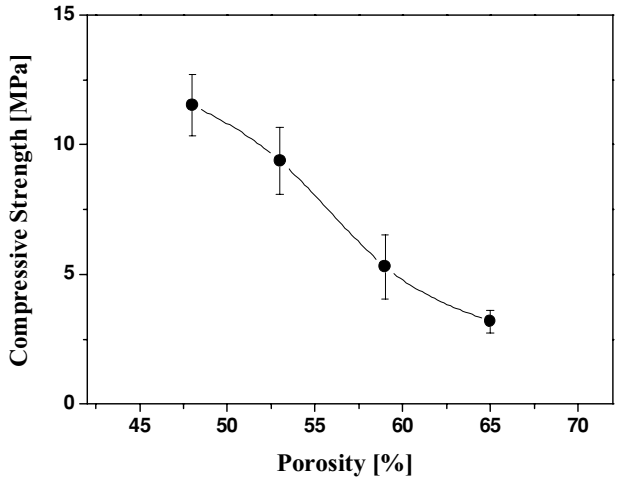

Fig. 3 Compressive strength of the HA scaffold, represented with respect to the porosity.

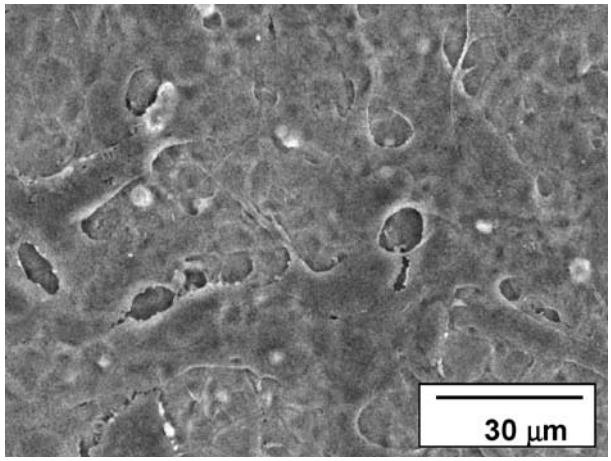

Fig. 4 Electron micrograph of the HOS cells grown on the HA scaffold after culturing for 4 days. Cells migrated deep into the scaffold and spread and grew well on the framework surface.

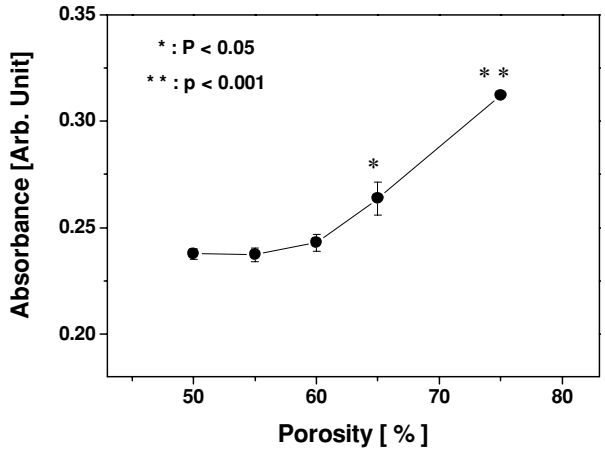

Fig. 5 Proliferation level of the HOS cells on the HA scaffold after culturing for 4 days, represented with respect to the porosity.

The osteoblastic phenotype expression of the cells was evaluated by measuring the ALP expression level after culturing for 14 days, since the ALP activity is regarded as an important marker characterizing osteoblastic or osteogenic cells undergoing the differentiation step [21, 22]. As the porosity increased, the ALP activity increased, as shown in Fig. 6. Compared to the cells on the sample with a porosity of 48%, those on the samples with higher porosities exhibited significantly higher ALP activity, suggesting that the cells grown on the scaffold with higher porosity exhibited enhanced functional activity.

With regard to the macrochanneled HA scaffolds, the benefits lie principally in the well-defined pore configuration, which can be controlled in a unique and simple way. In this study, the porosity was varied from 48 to 73%, while maintaining a predefined pore size (∼450 μm), and the effects of porosity on the mechanical and cellular responses were

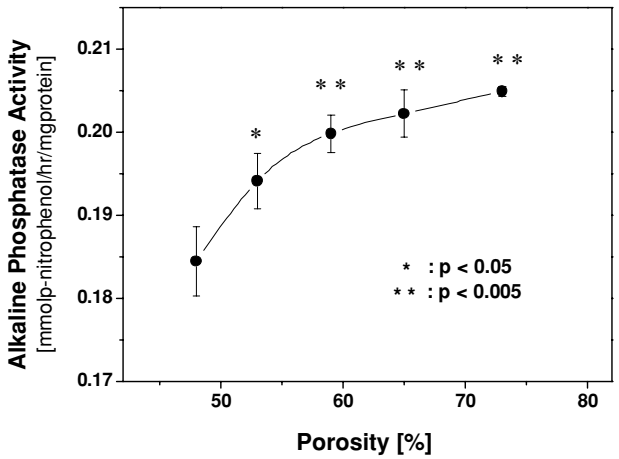

Fig. 6 Alkaline phosphatase (ALP) activity of the HOS cells on the HA scaffolds after culturing for 14 days, represented with respect to the porosity.

investigated. Based on the change in mechanical and biological data on the HA scaffolds with respect to porosity, the porosity range should be adjusted to fit the biological and mechanical properties required for specific applications, since both of these properties vary dissimilarly with regard to the porosity. However, all of the HA scaffolds fabricated within the porosity range of 48–65% are considered to posses sufficient strength (11.5–3.2 MPa) for use as hard tissue scaffolds, when considering that the compressive strength of the cancellous bone was approximately 2–12 MPa [23].

4. Conclusion

Hydroxyapatite (HA) porous scaffolds with macrochanneled pores were fabricated via a hybrid procedure of extrusion and lamination method. The macrochanneled pores and the HA framework were formed by a series of processes involving the stacking of thermoplastic carbon and HA filaments, the subsequent removal of the carbon black with thermal treatment, and final densification of the HA. The macrochanneled HA constituted a well-defined pore configuration with porosities of 48–73% at a pore size of approximately 450 μm. The compressive strength of the scaffolds decreased from 11.5 to 3.2 MPa as the porosity increased. At the same time, the cell viability and expression of osteoblastic phenotype (alkaline phosphatase) were significantly improved as the porosity increased.

Acknowledgments This work was supported by a grant of the Korea Health 21 R&D Project, Ministry of Health & Welfare, Republic of Korea (02–PJ3–PG6–EV11–0002).

References

1. L. L HENCH. *J. Amer. Ceram. Soc.* **74** (1991) 1487.
2. H. C. CAMERAN, I. PILLAR and R. M. MACNAB, *J. Biomed. Mater. Res.* **11** (1977) 179.
3. R. Z. LEGEROS and J. P LEGEROS, Dense Hydroxyapatite, in An Introduction to Bioceramics, Advanced Series in Ceramics, edited by L. L. Hench and J. Wilson (World Scientific, Singapoer, 1993) Vol. 1, p. 139.
4. D. M. ROY and S. K. LINNEHAN, *Nature* **247** (1974) 220.
5. C. LAVERNIA and J. M. SCHOENUNG, *Am. Ceram. Soc. Bull.* **70** (1991) 95.
6. T. S. B. NARASARAJUA and D. E. PHEBE, *J. Mater. Sci.* **31** (1996) 1.
7. M. JARCHO, *Clin. Orthop. Relat. Res.* **157** (1981) 259.
8. E. TSURUGA, H. TSURUGA, H. ITOH, Y. WAKISAKA and Y. KUKOKI, *J. Biochem.* **121** (1977) 317.
9. H. M. ROSEN, *Plast. Reconstr. Surg.* **83** (1989) 985.
10. N. PASSUTI, G. DACULSI, J. M. ROGEZ, S. MARTIN and J. V BAINVEL, *Clin. Orthop. Relat. Res.* **248** (1989) 169.
11. D. M. LIU, *Biomaterials* **17** (1996) 1955.
12. M. FABBRI, B. C. CELOTTI and A. RAVAGLIOLI, *Biomaterials* **15** (1994) 474.
13. D. M. LIU, *J. Mater. Sci. Lett.* **15** (1996) 419.
14. A. SLOSARCZYK, *Powder Metall. Int.* **21** (1989) 24.
15. H. W. KIM, S. Y. LEE, C. J. BAE, Y. J. NOH, H. E. KIM, H. M. KIM and J. S. KO, *Biomaterials* **24** (2003) 3277.
16. T. M. G. CHU, J. W. HOLLISTER and S. E. FEINBERG, *J. Mater. Sci-Mater M.* **12** (2001) 471.
17. T. M. G. CHU, D. G. ORTON, S. J. HOLLISTER, S. E. FEINBERG and J. W. HALLORAN, *Biomaterials* **23** (2002) 1283.
18. I. ZEIN, D. W HUTMACHER, K. C. TAN and S. H. TEOH, *Biomaterials* **23** (2002) 1169.
19. Y. H. KOH, H. W. KIM, H. E. KIM and J. W. HALLORAN, *J. Amer. Ceram. Soc.* **86** (2003) 2027.
20. Y. H. KOH, H. W. KIM, H. E. KIM and J. W. HALLORAN, *J. Amer. Ceram. Soc.* **85** (2002) 2578.
21. H. W. KIM, H. E. KIM, V. SALIH and J. C. KNOWLES, *J. Biomed. Mater. Res. A.* **68A** (2004) 522.
22. S. OZAWA and S. KASUGAI, *Biomaterials* **17** (1996) 23.
23. P. H. F. NICHOLSON, X. G. CHENG, G. LOWET, S. BOONEN, M. W. J. DAVIE, J. DEQUEKER and G. VAN DER PERRE, *Med. Eng. Phys.* **19** (1997) 729.